



HAL
open science

Retrovirus-Based Virus-Like Particle Immunogenicity and Its Modulation by Toll-Like Receptor Activation

Fabien Pitoiset, Thomas Vazquez, Béatrice Levacher, Djamel Nehar-Belaid, Nicolas Derian, James Vigneron, David Klatzmann, Bertrand Bellier

► **To cite this version:**

Fabien Pitoiset, Thomas Vazquez, Béatrice Levacher, Djamel Nehar-Belaid, Nicolas Derian, et al.. Retrovirus-Based Virus-Like Particle Immunogenicity and Its Modulation by Toll-Like Receptor Activation. *Journal of Virology*, 2017, 91 (21), pp.e01230-17 10.1128/JVI.01230-17 . hal-01675244

HAL Id: hal-01675244

<https://hal.sorbonne-universite.fr/hal-01675244>

Submitted on 4 Jan 2018

HAL is a multi-disciplinary open access archive for the deposit and dissemination of scientific research documents, whether they are published or not. The documents may come from teaching and research institutions in France or abroad, or from public or private research centers.

L'archive ouverte pluridisciplinaire **HAL**, est destinée au dépôt et à la diffusion de documents scientifiques de niveau recherche, publiés ou non, émanant des établissements d'enseignement et de recherche français ou étrangers, des laboratoires publics ou privés.

1 **Retrovirus-based Virus-Like Particle Immunogenicity and its Modulation by**
2 **Toll-Like Receptor Activation**

3
4
5 Fabien Pitoiset ^{a, b}, Thomas Vazquez ^{a, b}, Beatrice Levacher ^{a, b, *}, Djamel Nehar-
6 Belaid ^{a, b, *}, Nicolas Dérian ^{a, b}, James Vigneron ^{a, b}, David Klatzmann ^{a, b, c}, Bertrand
7 Bellier ^{a, b, c, #}.

8
9 ^a Sorbonne Universités, UPMC Univ Paris 06, UMRS_959, I³, Paris, France

10 ^b INSERM, UMR_S 959, Paris, France

11 ^c AP-HP, Groupe Hospitalier Pitié-Salpêtrière, Department of Biotherapies and the
12 Clinical Investigation Center in Biotherapy, Paris, France

13 * Authorship equal contribution

14
15 Running Title: Improvement of retrovirus-derived VLP immunogenicity by TLR ligand

16
17 # Address correspondence to Bertrand Bellier: bertrand.bellier@upmc.fr

18
19 Word counts: abstract: 180 words, importance: 121 words, text: 5434 words.

20 **Abstract**

21 Retrovirus-derived virus-like particles (VLPs) are particularly interesting vaccine
22 platforms as they trigger efficient humoral and cellular immune responses and can be
23 used to display heterologous antigens. In this study, we characterized the intrinsic
24 immunogenicity of VLPs and investigated their possible adjuvantization by
25 incorporation of toll-like receptor (TLR) ligands. We designed a non-coding single-
26 stranded RNA (ncRNA) that could be encapsidated by VLPs and induce TLR7/8-
27 signaling. We found that VLPs efficiently induce *in vitro* dendritic cell activation, which
28 can be improved by ncRNA encapsidation (_{ncRNA}VLPs). Transcriptome studies of
29 dendritic cells harvested from the spleen of immunized mice identified antigen
30 presentation and immune activation as the main gene expression signatures induced
31 by VLPs, while TLR signaling and Th1 signatures characterize _{ncRNA}VLPs. *In vivo* and
32 compared with standard VLPs, _{ncRNA}VLPs promoted Th1 responses and improved
33 CD8+ T cell proliferation in a MyD88-dependent manner. In an HIV vaccine mouse
34 model, HIV-pseudotyped _{ncRNA}VLPs elicited stronger antigen-specific cellular and
35 humoral responses than VLPs. Altogether our findings provide molecular evidence
36 for a strong vaccine potential of retrovirus-derived VLPs that can be further improved
37 by harnessing TLR-mediated immune activation.

38 **Importance**

39 We previously reported that DNA vaccines encoding antigens displayed in/on
40 retroviral VLPs are more efficient than standard DNA vaccines at inducing cellular
41 and humoral immune responses. We aimed to decipher the mechanisms and
42 investigated the VLPs immunogenicity independently of the DNA vaccination. We
43 show that VLPs have the ability to activate antigen-presenting cells directly, thus
44 confirming their intrinsic immunostimulatory properties and their potential to be used
45 as an antigenic platform. Notably, this immunogenicity can be further improved
46 and/or oriented by the incorporation into VLPs of ncRNA, which provides further TLR-
47 mediated activation and Th1-type CD4+ and CD8+ T cell response orientation. Our
48 results highlight the versatility of retrovirus-derived VLP design and the value of
49 using ncRNA as an intrinsic vaccine adjuvant.

50

51 **Introduction**

52 The development of successful vaccines against viruses such as HIV or HCV
53 requires new approaches, and in particular vaccines that are able to elicit both
54 cellular and humoral immune responses contributing to protective immunity. A major
55 advance in vaccine development has been the production of antigens as virus-like
56 particles (VLPs) that mimic the overall structure of virus particles, without the
57 requirement of containing infectious genetic material. VLP designs are based on the
58 observation that expression of the capsid proteins of many viruses leads to the
59 spontaneous assembly of pseudo-particles with an authentic conformation, but
60 devoid of DNA or RNA viral genome, thus rendering them replication incompetent. In
61 addition to safety, their particulate nature, highly repetitive structure and ability to
62 activate innate immune cells explain the strong immunogenicity of VLPs (1),(2) and
63 their success in vaccine development (3). To date, VLPs have been used as
64 prophylactic vaccines against homologous viral diseases, such as hepatitis B or
65 papillomavirus infection, and have shown excellent efficacy and safety profiles. VLPs
66 have also been proposed as an antigen carrier platform for heterologous vaccination.
67 The insertion of target antigens into viral structural proteins able to self-assemble has
68 been the most common method of producing these chimeric VLPs. Different VLPs
69 have been adapted for this purpose (4) and there have been notable successes in
70 developing vaccines, notably against malaria (5).

71 We previously developed recombinant murine leukemia retrovirus–based VLPs (MLV
72 VLPs) as a vaccine platform. These VLPs are made of the Moloney MLV-Gag capsid
73 proteins that can self-assemble into pseudo-particles in host cells by budding at the
74 plasma membrane. Target antigens can be inserted either into the particles by fusion
75 with Gag proteins or displayed at their surface by co-expression of Gag with
76 recombinant protein fused to the transmembrane domain of the vesicular stomatitis
77 virus glycoprotein (VSV-G) (6). We demonstrated that the expression of antigens both
78 in and on VLPs significantly improves their immunogenicity, favoring the induction of
79 both B- and T-cell–mediated immunity in a context of DNA vaccination. Indeed,
80 plasmid DNA encoding chimeric VLPs induces higher cellular and humoral immune
81 responses against target antigens than a control DNA vaccine encoding antigens not
82 associated with VLPs (7),(8),(9),(10).

83 In order to favor vaccine-induced Th1 responses, which play a critical role in antiviral
84 immunity (11),(12), stimulation of Toll-like receptor (TLR) ligands (13) has been
85 investigated (14). TLRs are receptors expressed by innate immune cells,
86 predominantly by antigen-presenting cells (APCs), and recognize various pathogen
87 components, such as proteins, nucleic acids or sugars, from viruses, bacteria or
88 parasites (15). Upon binding to pathogen-associated molecular patterns (PAMPs),
89 TLR signaling activates the APCs resulting in production by dendritic cells (DCs) of
90 cytokines, notably IL-6, IL-12 and IFN- γ (14), increased co-stimulatory molecule
91 expression and enhanced capacity to present and cross-present antigens on MHC
92 class I molecules (16),(17). Among the different TLRs that are able to recognize
93 pathogenic nucleic acids, TLR7, 8 and 9 have been extensively studied for the
94 induction of Th1 responses for anti-tumor and anti-viral vaccination (17),(18),(19),(20).

95 Here, we designed a new strategy to incorporate non-coding RNA (ncRNA), which
96 acts as a TLR7/8 ligand in MLV-derived VLPs and is characterized by its impact on
97 their immune properties. We compared VLPs and _{ncRNA}VLPs for their capacity to
98 activate DCs, to prime CD8⁺ and CD4⁺ T cell responses and to generate anti-HIV
99 immune responses in mice. Collectively, our results demonstrate that MLV-derived
100 VLPs have intrinsic adjuvant properties that can be further improved by incorporation
101 of ncRNA.

102

103 **Material and Methods**

104 **Cell lines**

105 HEK293T cells (CRL-1573; ATCC) were grown in Dulbecco's modified Eagle
106 medium (DMEM) supplemented with 2 mM L-glutamine, 100 U/mL penicillin, 100
107 μ g/mL streptomycin (all from Life Technologies, Cergy Pontoise, France) and 10%
108 heat-inactivated fetal calf serum.

109 **Mice**

110 6- to 7-week-old female C57BL/6J mice were from Janvier Labs (Le Genest-Saint-
111 Isle, France). OT-I (C57BL/6-Tg(TcraTcrb)1100Mjb), OT-II (C57BL/6-
112 Tg(TcraTcrb)425Cbn) and MyD88^{-/-} (on a C57BL/6 background; (21)) mice were bred

113 at the CEF animal facility at the Pitié-Salpêtrière Hospital. Mice were maintained
114 under specific pathogen-free conditions, and manipulations were performed
115 according to European Economic Community guidelines and approved by the local
116 ethics committee (ce5/2009/042).

117 **Plasmid DNA**

118 pGag encodes the Moloney MLV-Gag under the CMV promoter. pGag is obtained by
119 deletion of Pol by PCR in the pBL35 (7) with insertion of the MluI restriction site at the
120 3' end of Gag before the terminal stop amino acid. For pGag-gp33-41, the
121 KAVYNFATC epitope (gp33-41), flanked upstream and downstream by 5 natively
122 neighboring amino acids as previously described (7), was added at the 3' end of the
123 MLV gag sequence in pGag. pBL196 encodes a fusion protein MLV-Gag-OVA. The
124 OVA sequence was synthesized (GenScript Corporation, Piscataway, NJ 08854,
125 USA) and inserted at the end of MLV-Gag with restriction sites (MluI/XbaI) in pGag.
126 pHCMV-VSV-G encoding VSV-G was previously described (22). pgp140-TM is a
127 synthetic plasmid under the EF1 α promoter encoding the GP140_{TM} fusion chimeric
128 protein. HIV Gp140 (Clade B, Strain JRFL) was fused after Lys-674 to the VSV-G
129 transmembrane domain (TM) by PCR insertion of the 49 amino acids from Ser-463 to
130 Lys-511. pncRNA was obtained by deleting the coding region from a CMV-GFP
131 retroviral transgene (kindly provided by FL Cosset) after digestion with EcoR1.

132 **Production of VLPs**

133 HEK-293T cells (ATCC/CRL-1573) (15×10^6 cells/175 cm² flask) were transfected
134 using a calcium phosphate protocol with 50 μ g of total plasmid DNA. For VLPs (i)
135 pGag and pHCMV-VSV-G or (ii) pGag-gp33-41 and pgp140-TM were used in a 2:1
136 ratio. For _{ncRNA}VLPs (i) pGag, pHCMV-VSV-G and pncRNA or (ii) pGag-gp33-41,
137 pgp140-TM and pncRNA were used in a 2:1:1 ratio. After 48 h, supernatants were
138 collected, filtered through 0.45 μ m pore-sized membranes and concentrated with
139 Centricon (Millipore, Molsheim, France). Then, supernatants were layered on top of a
140 sucrose step gradient (2.5 mL 35% and 2.5 mL 50%) and centrifuged at 100,000 g
141 for 2 h at 4°C. The interface was collected and washed with PBS in an identical
142 centrifugation step to eliminate remaining sucrose. Quantification of VLPs was
143 performed by BCA (Thermo Fisher Scientific, USA).

144 **Endotoxin quantification**

145 Endotoxin levels in VLP preparations were quantified with the LAL Chromogenic
146 Endotoxin Quantitation Kit (Thermo Fisher Scientific), following manufacturer's
147 instructions. Absorbance was read at a wavelength of 405 nm in a DTX-800
148 Microplate Reader (Beckman Coulter, USA).

149 **Detection of ncRNA in VLPs**

150 Purified VLPs and ncRNA VLPs were incubated at 75°C for 10 min to release RNA and
151 treated with DNase I RNase-free (Invitrogen, France) for 30 min at room
152 temperature. As a control, total RNA from HEK-293T cells ($3 \cdot 10^6$ cells) was isolated
153 by using RNeasy Mini Kits (Qiagen, France). cDNA synthesis from HEK-293T or
154 VLPs was performed in triplicate using Superscript III (Invitrogen, France) according
155 to the manufacturer's instructions, using primers specific to the MLV LTR region.
156 Forward primer 5'- ATA GAC TGA GTC GCC CGG-3' and reverse primer 5'- AGC
157 GAG ACC ACA AGT CGG AT-3' were synthesized by Sigma-Aldrich. Quantitative
158 PCR was performed using the 7500 Fast Real-Time PCR System (Life Technologies,
159 France) with FG, Power Sybr master mix (Life Technologies, France).

160 **Quantification of total RNA in VLPs**

161 VLPs were transferred in Trizol Reagent (Life Technologies, France) and extraction
162 was performed according to the manufacturer's instructions. Phase Lock Gel
163 (5PRIME) was used to separate phases. Extracted RNA was treated with the DNA-
164 free Kit (Ambion). Yields of RNA from VLPs were determined by the Quant-iT™
165 RiboGreen RNA Reagent (Invitrogen). Escherichia coli 16S and 23S rRNA provided
166 by the manufacturer were used as controls.

167 **Assay of murine bone marrow–derived dendritic cell activation**

168 Bone marrow cells collected from tibias and femurs of C57Bl/6 or MyD88^{-/-} mice were
169 cultured for 9 days in IMDM medium (Life Technologies, Cergy Pontoise, France)
170 supplemented with 2 mM L-glutamine, 100 U/mL penicillin, 100 µg/mL streptomycin
171 (all from Life Technologies, Cergy Pontoise, France), 10% heat-inactivated fetal calf
172 serum and GM-CSF (supernatant of J558 hybridoma kindly provided by D. Gray,
173 University of Edinburgh, Edinburgh, U.K.). Fresh medium was added every 3 days.

174 At day 9, differentiated BMDCs were cultured for 24 additional hours in the presence
175 of VLPs, *ncRNA*VLPs or medium alone as control. Expression of activation markers
176 was analyzed by flow cytometry.

177 **Transcriptome analysis of dendritic cells**

178 C57Bl/6 mice were i.v. injected with 25 µg of VSV-G-pseudotyped VLPs, *ncRNA*VLPs
179 or with PBS in the control group. Six hours later the mice were sacrificed and DCs
180 were isolated from spleen using magnetic separation with CD11c-specific
181 microbeads (Miltenyi Biotec, Paris, France). Purity of sorting cells was verified by
182 flow cytometry and cells were frozen in Trizol after 2 washes in PBS. RNA was
183 isolated using the RNeasy Mini kit (QIAGEN). RNA yield was assessed using a
184 NanoDrop ND-1000 spectrophotometer (Thermo Fisher Scientific) and RNA integrity
185 was confirmed by using an Agilent Bioanalyzer (Agilent Technologies) with a
186 minimum RNA integrity number (RIN) of 9. Total RNA was amplified and converted to
187 biotinylated cRNA according to the manufacturer's protocol (Illumina TotalPrep RNA
188 Amplification Kit; Ambion). Four biological replicates were hybridized to the Sentrix
189 BeadChips Array mouse WG-6 v2 (Illumina). Data extraction was done with
190 BeadStudio software and expression levels were normalized by a quantile method
191 using the limma R package. The quality of the dataset was checked by using an
192 unsupervised clustering analysis of experimental groups compared with the control.
193 At this step, one control mouse was excluded from analyses because of pre-analytic
194 statistical tests (Principal Variance Component Analysis) showing that some
195 experimental issues were responsible for an external variability source. Gene
196 ontology (GO)-based signatures were tested for their significance on our microarray
197 data using Gene Set Enrichment Analysis (GSEA) software and statistically
198 significant molecular signatures (false discovery rate (FDR) $q.value < 0.05$) were
199 selected. Molecular signatures that were differentially modulated in VLP or *ncRNA*VLP
200 groups compared with the PBS group were mapped using Cytoscape software (23)
201 with the "Enrichment map" plugin (24). Each dot represent a molecular signature from
202 the Gene Ontology Database that is significantly enriched compared to the PBS
203 group. If two of these signatures show a strong overlap between their genes, they are
204 linked by an edge (based on the Jaccard similarity index), and the length of this edge
205 depends on the number of genes shared by the two signatures (the more genes they
206 share, the shorter the edge is). Signatures specifically regulated in the *ncRNA*VLPs and

207 not shared with the VLPs were identified to characterize the specific ncRNA impact
208 on DCs. Heatmaps were generated by using heatmap.2 R package software to show
209 the individual gene expression in signatures of interest. Raw microarray data have
210 been deposited in NCBI's Gene Expression Omnibus (GEO) and are accessible
211 through GEO series accession number GSE70557
212 (<http://www.ncbi.nlm.nih.gov/geo/query/acc.cgi?acc=GSE70557>).

213 **Quantitative PCR**

214 Complementary DNA was generated using SuperScript VILO (Life Technologies,
215 France) and performed reverse transcription according to the manufacturer's
216 instructions. Quantitative PCR was performed using the 7500 Fast Real-Time PCR
217 System (Life Technologies, France) with Fast Master Mix (Life Technologies, France)
218 and TaqMan gene expression assay probes (Life Technologies, France). The probe
219 IDs are Irf1: Mm01288580_m1, Irf7: Mm00516793_g1, Mx2: Mm00488995_m1,
220 Relb: Mm00485664_m1, Rsad2: Mm00491265_m1, Slc2a6: Mm00554217_m1,
221 Traf6: Mm00493836_m1, Xcl1: Mm00434772_m1 and 18S: Mm03928990_g1.
222 qPCRs were performed in triplicate and the mRNA levels were normalized to that of
223 GAPDH mRNA and 18S mRNA.

224 ***In vitro* proliferation of antigen-specific CD8⁺ T cells**

225 Spleen cells were collected from C57BL/6, MyD88^{-/-} and OT-I mice. DCs from
226 C57BL/6 and MyD88^{-/-} mice were isolated by magnetic sorting with CD11c
227 microbeads (Miltenyi Biotec). OT-I CD8⁺ T cells were isolated by negative selection
228 using biotin-conjugated antibodies specific for CD11c, CD11b and B220 (all from BD
229 Biosciences, Pont-de Claix, France) plus anti-biotin microbeads (Miltenyi Biotec) and
230 stained with CFSE (Life Technologies). In a 96-well plate, 2x10⁵ OT-I CFSE⁺ splenic
231 cells were cultured in RPMI medium supplemented with 2 mM L-glutamine, 100 U/mL
232 penicillin, 100 µg/mL streptomycin (all from Life Technologies, Cergy Pontoise,
233 France) and 10% heat-inactivated fetal calf serum, with 4x10⁴ CD11c⁺ cells (ratio
234 5:1) from C57BL/6 or MyD88^{-/-} mice in the presence of 5 µg of VSV-G-pseudotyped
235 Gag-OVA VLPs or ncRNA VLPs, or medium for control. After 3 days, proliferation and
236 activation of OVA-specific CD8⁺ T cells were analyzed by flow cytometry.

237 ***In vivo* proliferation of CD8⁺ or CD4⁺ T cells**

238 C57Bl/6 or MyD88^{-/-} mice were immunized by i.v. injection of 1 µg of VSV-G-
239 pseudotyped Gag-OVA VLPs or _{ncRNA}VLPs or PBS in the control group. 6 hours later,
240 CFSE-stained OT-I or OT-II spleen cells containing 1.5x10⁶ transgenic cells
241 (proportion measured by flow cytometry) were i.v. injected. After 3 or 5 days, spleens
242 were collected and proliferation of OT-I or OT-II transgenic CFSE+ cells was
243 evaluated by flow cytometry.

244 **Flow cytometry**

245 Immunostaining for flow cytometry was performed with the following mAbs: V500-
246 conjugated anti-CD4, AF700-conjugated anti-CD8, V500-conjugated anti-IA/E, biotin-
247 conjugated anti-CD80, biotin-conjugated anti-CD44, efluor450-conjugated anti-CD86,
248 APC-conjugated anti-Tbet, PE-conjugated anti-GATA3 (all from BD Biosciences),
249 APC-conjugated anti-CD11c and APC-conjugated anti-Vα2 (both from eBiosciences).
250 Biotin-conjugated antibodies were detected with PECy7-conjugated streptavidin
251 (eBioscience). In *in vitro* assays, 7-AAD viability dye was added to exclude dead cells
252 from the analysis. All cytometry experiments were performed with a BD™ LSRII
253 cytometer and data were analyzed using FlowJo software (Treestar).

254 **HIV immunizations**

255 6-week-old C57BL/6 or MyD88^{-/-} female mice were immunized s.c. at weeks 0, 2 and
256 4 with 25 µg of HIV-gp140 pseudotyped Gag-gp33-41 VLPs or _{ncRNA}VLPs. At weeks
257 6 and 12, sera were collected from blood samples to analyze antibody responses. At
258 week 12, mice were sacrificed to analyze cellular immune responses.

259 **Anti-HIV humoral immune response**

260 HIV-specific IgG antibody concentrations in the sera were evaluated by gp140-
261 specific ELISA. Gp140 protein (kindly provided by R. Wyatt, US) was coated at 0.5
262 µg/mL O/N at 4°C before adding diluted sera for 2 hours at RT. Anti-mouse IgG
263 coupled to horseradish peroxidase (HRP; Dako, Hamburg, Germany) was then
264 added for 1 hour RT. After washing, TMB (eBioscience) was added and absorbance
265 was read at 405 nm. 2G12 antibody (Polymun Scientific, Austria) was used as
266 standard for determination of HIV-specific antibody concentration.

267 **Anti-HIV cellular immune response**

268 Splens were collected and specific IFN- γ production by T cells was determined in a
269 standard ELISPOT assay (Mabtech). Briefly, 5×10^5 spleen cells were restimulated for
270 24 h at 37°C in 5% CO₂ with 10 μ g/mL of gp33-41 peptide or 10 ng/well of gp140-
271 pseudotyped lentiviral particles made of HIV Gag. Medium alone and concanavalin A
272 (ConA; Sigma-Aldrich) at 3 μ g/mL were used as negative and positive controls,
273 respectively. Spots were counted with an AID ELISPOT reader (ELR03; AID,
274 Germany). Results were expressed as spot-forming units (SFUs) per 10^6 cells.

275

276 **Results**

277 **ncRNA encapsidation into VLPs**

278 The ncRNA plasmid derived from a retroviral vector from which the coding reporter
279 gene was deleted. Only the flanking regions (R, U5 from 5'-LTR and U3, R, U5 from
280 3'-LTR), the tRNA primer-binding site (PBS), the retroviral packaging signal
281 sequence (ψ) and the polypurine tract (PPT) were functional (Fig. 1A). As a result,
282 the ncRNA plasmid produces RNA molecules that do not encode specific proteins
283 but can be incorporated into retroviral particles by interactions between Gag and ψ
284 elements during the packaging process in addition to cellular RNAs (Fig. 1B). The
285 presence of ncRNA was tested by RT-qPCR on pseudo-particles purified from
286 H293T cells transfected with plasmid DNA encoding MLV-Gag, VSV-G envelope
287 glycoproteins, and ncRNA or not. Specific detection of ncRNA was observed in
288 pseudo-particles produced in the presence of ncRNA plasmid ($_{ncRNA}$ VLPs), while the
289 signal detected in VLPs produced in the absence of the ncRNA plasmid was
290 equivalent to the background (Fig. 1C). Similar results were observed in pseudo-
291 particles produced with chimeric MLV-Gag proteins fused with OVA or gp33-41
292 antigens (data not shown), demonstrating that ncRNA was efficiently encapsidated in
293 the different recombinant VLPs used in this study. qPCR assay was also performed
294 without the reverse transcription step in order to evaluate the eventual presence of
295 contaminating ncRNA-encoding plasmid DNA in our preparations. Positive results
296 were obtained but level of plasmid DNA was around 1000 times lower than signal
297 observed after reverse transcription.

298 Wondering if the presence of the ncRNA into the particles could modify the quantity
299 of cellular RNA packaged, we compared the total RNA quantity in *ncRNA*VLP and VLP
300 preparations and observed very similar quantities in both types of VLPs (mean of 593
301 ng/μg for *ncRNA*VLPs, 528 ng/μg for VLPs). This suggests that the incorporation of
302 ncRNA in VLPs does not significantly modify the total quantity of RNA carried by the
303 particles but impact its quality since *ncRNA*VLPs specifically harbor RNA of viral origin
304 in addition to cellular RNAs. Also, to exclude the possibility that endotoxins could play
305 a role in the VLP effect described later on, we assessed the possible LPS
306 contamination by performing a Limulus amoebocyte lysate (LAL)-based assay on
307 different preparations of VLPs. Results show that there are low endotoxin levels in
308 our VLP preparations, lower actually than in a commercial OVA protein batch used
309 as control (Fig. 1E). Importantly the endotoxin levels measured in VLPs and
310 *ncRNA*VLPs are very similar, thus guaranteeing that the comparison between the two
311 types of VLPs is not biased by endotoxin contamination.

312 **ncRNA carried in VLPs increases dendritic cell activation in a MyD88-** 313 **dependent manner**

314 To evaluate the ability of ncRNA to improve the immunogenicity of VLPs, we
315 compared the capacity of VLPs and *ncRNA*VLPs to activate murine DCs. C57Bl/6
316 immature BMDCs were cultured in the presence of 1, 5, or 10 μg of VLPs ± ncRNA
317 for 24 hours and expression of CD80 (Fig. 2A, 2C and 2E) and CD86 (Fig. 2B, 2D
318 and 2F) costimulation molecules were analyzed by flow cytometry. Medium alone,
319 R848 (TLR7 ligand) and LPS (TLR4 ligand) were used as negative and two positive
320 controls, respectively. We observed a dose-dependent activation of BMDCs with
321 standard VLPs (in the absence of viral RNA), demonstrating their intrinsic
322 immunogenicity and confirming our previous results observed with human DCs (10).
323 Moreover, a significant higher expression of both CD80 and CD86 was observed with
324 *ncRNA*VLPs as compared with standard VLPs (Fig. 2E and 2F), demonstrating the
325 adjuvant properties of encapsidated ncRNA.

326 Engagement of the TLR pathways was evaluated by conducting similar experiments
327 with BMDCs from mice deficient for the myeloid differentiation primary response
328 gene 88 (MyD88^{-/-} mice), which is involved in the signaling pathways of most of the
329 TLRs. As expected, R848 had no activation effect in MyD88^{-/-} BMDCs while LPS,

330 which is known to induce both a MyD88-dependent and -independent pathway, still
331 induced cell activation (Fig. 2I-J). Interestingly, very weak activation was observed
332 with VLPs in MyD88^{-/-} BMDCs and was not significantly increased with ncRNA VLPs
333 (Fig. 2G-L). Therefore, we first conclude that VLPs alone are able to trigger a
334 MyD88-dependent pathway, partly explaining their immunogenicity and suggesting
335 that VLPs are recognized by some TLRs. Secondly, as no effect of ncRNA was
336 observed on activation of MyD88^{-/-} BMDCs, this confirms that the increased activation
337 of wild-type BMDCs is mediated by TLR activation by ncRNA, likely TLR7 and/or
338 TLR8.

339 **Transcriptome analysis of dendritic cells activated by VLPs or ncRNA VLPs**

340 In order to better characterize the intrinsic immunogenicity of MLV-derived VLPs and
341 the mechanisms related to DC activation by ncRNA, we performed a transcriptome
342 analysis of sorted CD11c⁺ cells from the spleen of C57Bl/6 mice 6 hours after
343 intravenous injection of VLPs or ncRNA VLPs. As expected a large set of shared genes
344 (n = 572) was differentially expressed in both VLP or ncRNA VLP groups. In contrast,
345 few genes (n = 169) were specifically modulated by ncRNA. Using unsupervised
346 analysis with multidimensional scaling, no efficient segregation between VLP and
347 ncRNA VLP groups were observed (not shown), confirming the high similarities between
348 the two groups.

349 However, based on the differentially expressed genes and Gene Set Enrichment
350 Analysis (GSEA), we identified signatures significantly regulated in VLP or ncRNA VLP
351 groups in comparison with controls. The results were mapped as a network of
352 signatures (nodes) related by similarity (edges) in which shared signatures and
353 specific ones of ncRNA VLPs were indicated in gray and red, respectively (Fig. 3A). As
354 expected, the two types of VLPs share common signaling pathways that are
355 organized in functional modules related to immunology, including immune response,
356 proteasome activity and viral processes (in gray). We focused on signatures that are
357 specifically enriched in the ncRNA VLP group, shown in red in Figure 3A. These specific
358 signatures were related to (i) RNA transport (ii) Th1 immune response and (iii) IFN-
359 γ /IL-4 secretion, , which is very consistent with the presence of ncRNA in VLPs and
360 its ability to polarize the immune responses. Three of the immune-related enriched
361 GO signatures are represented in Figure 3B, confirming the ability of ncRNA to

362 activate DCs and activate TLR signaling, and revealing their capacity to induce Th1-
363 biased immune responses, as shown for example by the increased expression of *Irf1*
364 (interferon regulating factor-1) and *Xcl1* genes, which are associated with Th1
365 responses. Notably, increased expression of eight important genes from the 3
366 selected signatures, including *Irf1* and *Xcl1*, was confirmed by RT-qPCR (Fig. 3C),
367 strengthening our results.

368 **ncRNA increases cross-presentation of antigens carried by VLPs**

369 We next considered the specific role of the carried ncRNA in antigen cross-
370 presentation and CD8⁺ T cell activation. *In vitro* T cell proliferation experiments were
371 performed with transgenic OT-I CD8⁺ T cells (specific for OVA257-264 peptide,
372 restricted to H2-K^b MHC class I molecules) co-cultured for 3 days with wild-type or
373 MyD88^{-/-} DCs in the presence of OVA-recombinant VLPs made of Gag-OVA fusion
374 proteins and carrying or not ncRNA. We observed that recombinant VLPs induced
375 specific proliferation of the TCR-transgenic CD8⁺ T cells, which was significantly
376 higher with _{ncRNA}VLPs compared with VLPs devoid of ncRNA (Fig. 4A). When the
377 experiments were performed with MyD88^{-/-} DC cells in presence of standard
378 recombinant VLPs, we observed similar levels of proliferation to those induced by
379 wild-type DCs, indicating that TLR recognition is not absolutely necessary for
380 induction of CD8⁺ T cell proliferation (Fig. 4B). Importantly, no significant
381 improvement of *in vitro* T cell proliferation was observed with _{ncRNA}VLPs in the
382 presence of MyD88^{-/-} DC cells, demonstrating that ncRNA requires MyD88-
383 dependent signals to express its adjuvant properties.

384 We tested the adjuvant effect of ncRNA on *in vivo* CD8⁺ T cell proliferation by
385 injecting OVA-recombinant VLPs or _{ncRNA}VLPs in C57BL/6 wild-type or MyD88^{-/-}
386 mice, injected 6 hours later with CFSE-stained OT-I T cells. Consistent with the *in*
387 *vitro* experiments, a significantly higher proliferation of transgenic OT-I CD8⁺ T cells
388 was observed at day 3 with the _{ncRNA}VLPs compared with VLPs (Fig. 4C and 4D),
389 confirming the ability of ncRNA molecules to amplify CD8⁺ T cell responses. In
390 contrast, no difference in CD8⁺ T cell proliferation was observed in MyD88^{-/-} mice
391 when VLPs and _{ncRNA}VLPs were compared (Fig. 4E), confirming the involvement of
392 TLR activation in the *in vivo* adjuvant effect of ncRNA.

393 **ncRNA improves antigen-specific CD4⁺ T cell activation and Th1 polarization**

394 We also considered the specific role of the carried ncRNA in CD4⁺ T cell activation
395 and differentiation. *In vivo* T cell proliferation experiments were performed with OVA-
396 specific transgenic OT-II CD4⁺ T cells. Interestingly, OVA-recombinant _{ncRNA}VLPs
397 significantly improved the proliferation of antigen-specific CD4⁺ T cells, as shown in
398 an adoptive transfer model with OT-II cells (Fig. 4F) and compared with VLPs. The
399 polarization of effector CD4⁺ T cells was investigated and intracellular staining of
400 Tbet and GATA3 transcription factors was performed. We observed a significant
401 increase of the ratio of the mean fluorescence intensities of Tbet and GATA3 in
402 divided CD4⁺ T cells from mice immunized with _{ncRNA}VLPs as compared with VLPs,
403 reflecting a Th1-biased polarization (Fig. 4G). Notably, these results were accordant
404 with the transcriptome analysis (Fig. 3B) and confirm the ability of ncRNA to promote
405 Th1 immune responses.

406 **ncRNA improves vaccine specific responses in mice**

407 Finally, we evaluated the impact of ncRNA in a vaccination model against HIV by
408 using MLV-derived VLPs pseudotyped with HIV-1 gp140 envelope glycoproteins. The
409 gp33-41 CD8⁺ T-cell specific model antigen was fused to MLV-Gag to evaluate
410 simultaneously the cross-priming efficiency. C57Bl/6 mice were immunized
411 subcutaneously three times every 2 weeks with HIV-pseudotyped recombinant VLPs
412 or _{ncRNA}VLPs (Fig. 5A) and T cell responses were measured at week 12 by IFN- γ
413 ELISPOT after restimulation either with gp33-41 or HIV-1 gp140 antigens. While
414 VLPs devoid of ncRNA generated modest but significant IFN- γ T cell immune
415 responses against gp33-41, _{ncRNA}VLPs significantly increased the responses (Fig.
416 5B). Adding ncRNA also significantly increased the gp140-specific IFN- γ T cell
417 immune responses (Fig. 5C), highlighting the adjuvant properties of ncRNA in
418 inducing HIV-specific Th1 immune responses in a vaccine approach. Importantly, the
419 improvement of CD4⁺ T cell immune responses by ncRNA was TLR-mediated since
420 no significant differences were observed between VLPs and _{ncRNA}VLPs when
421 experiments were conducted in MyD88^{-/-} mice (Fig. 5B-C).

422 Antibody responses were evaluated by measuring the anti-gp140 specific antibody
423 concentration in the serum of vaccinated mice, either at week 6 (Fig. 5D) or at week
424 12 (Fig. 5E) to assess its long-term persistence. At the early time point after
425 immunizations, high antibody concentrations were detected but no difference was

426 observed between the two groups (Fig. 5D). In contrast, at week 12, anti-gp140
427 antibody concentration had dramatically dropped in the group immunized with VLPs,
428 while mice immunized with _{ncRNA}VLPs still presented high levels of anti-gp140
429 antibodies (Fig 5E), revealing a capacity of the ncRNA adjuvant to maintain HIV-
430 specific antibody levels in the sera of immunized mice.

431

432 **Discussion**

433 VLPs are considered as highly immunogenic vaccines and are used as an antigenic
434 platform to increase the immunogenicity of antigens (2). Here, we studied the
435 immunogenic properties of MLV-derived VLPs and propose an adjuvant strategy to
436 increase their immunogenicity. We confirmed the ability of these VLPs to induce
437 activation of antigen-presenting cells. Indeed, efficient uptake of VLPs and activation
438 of murine BMDCs were demonstrated, which represent the prerequisite for the high
439 immunological activity of recombinant VLPs and confirm our previous observations
440 with human monocyte-derived DCs (10). DC activation was confirmed with VLPs
441 highly purified by anion exchange chromatography on Q Sepharose (data not
442 shown), demonstrating that their immunogenicity is not due to the presence of
443 contaminants in the VLP preparation, which was already reported in baculovirus-
444 expressed VLPs and may partially explain the enhanced immunogenicity of these
445 types of VLPs (25). By contrast, it is well known that in the human cell lines production
446 systems, human surface proteins are incorporated in the membrane of VLPs, and
447 these proteins probably play a role in the observed immunogenicity of particles, as it
448 has been shown for tetraspanins for example (26). Moreover, we demonstrated that
449 MLV VLPs induce efficient cross-presentation as shown by *in vitro* and *in vivo*
450 proliferation of CD8+ T cells against displayed antigens. Consistent with our findings,
451 other groups previously demonstrated that antigens carried by different VLPs,
452 including HBs- and HCV-derived VLPs, can be efficiently cross-presented by DCs
453 (27)(28).

454 Several mechanisms could explain the intrinsic adjuvant-like properties of MLV VLPs.
455 Based on transcriptome analyses, we observed that MLV VLPs positively regulate
456 numerous immunological signatures related to the immune response, proteasome
457 activity and viral processes (Fig. 3A). Interestingly, experiments conducted with

458 MyD88^{-/-} DCs revealed that the Toll-like receptor pathways are also involved in VLP
459 immunogenicity (Fig. 2). We observed a significant increase of MyD88 and TLR2
460 gene expression in DC transcriptome studies that was confirmed by TLR2 activation
461 using the Invivogen TLR screening[®] assay (data not shown). However, even if TLR
462 seems to be involved in VLP-induced DC activation, MyD88 signaling is not sufficient
463 to fully explain the immune properties of MLV VLPs, since T-cell immune responses
464 observed in MyD88^{-/-} and wild-type mice after OVA-recombinant VLP immunization
465 were equal (Fig. 4). Other mechanisms could be linked to the high immunogenicity of
466 MLV VLPs. Notably, disruption of the structure of VLPs by boiling them for 10
467 minutes led to a dramatic loss of DC activation (data not shown), demonstrating that
468 the particular nature of VLPs confers them intrinsic adjuvant properties. However, we
469 assume that VLPs immunogenicity may be overestimated since VLPs were prepared
470 in human 293T cells and tested in mice.

471 Otherwise, we describe in this study a novel adjuvant strategy for vaccination with
472 MLV VLPs using ncRNA, a non-coding single-stranded RNA molecule capable of
473 being packaged in the particles. As it is well known that numerous host cell RNAs
474 can be encapsulated in MLV particles (29)(30), we postulated that ncRNA can be
475 enriched in VLPs due to the presence of the *psi* sequence, and can express adjuvant
476 properties after binding to TLR7 and/or TLR8. TLR7/8 ligands have already shown
477 great results as immunomodulating therapeutic agents (31)(32) and are very
478 promising vaccine adjuvants, including against HIV (33)(34). Consistently with these
479 results, TLR7/8 agonists have been shown to efficiently activate and induce cytokine
480 secretion by DCs, in a MyD88-dependent way (35)(36)(37). Here, we demonstrated *in*
481 *vitro* and *in vivo* that ncRNA improves VLP immunogenicity after TLR recognition.
482 Transcriptome analyses reveal that ncRNA-induced DC maturation is linked to the
483 NF-κB signaling pathway, as shown by the increased expression of Traf6, Batf,
484 Batf2, RelB in murine DCs, and a significant modulation of the TLR signaling related
485 genes (Fig. 3B-C). Among those genes, Rsad2 (or Viperin) which has already been
486 shown to promote interferon-β secretion in response to TLR7 ligand (38) and acts on
487 antigen presentation (39) as shown by ubiquitin D (Ubd) gene upregulation in splenic
488 DCs was up-regulated. We also observed a significant increase in numerous genes
489 involved in the response to interferons such as Mx2, Oas1, Oas2, Socs3, Irf7 and
490 several other interferon-inducible genes, suggesting that ncRNA triggers interferon

491 secretion. Interestingly, these genes have also been reported by Pulandran et al. to
492 play a key role in vaccine responses against commercialized vaccines and may be
493 predictive for an efficient vaccine response (40–43).

494 TLR7/8 ligands have been especially used for their capacity to enhance CD8+ T cell
495 responses against numerous antigens (33),(44),(45),(46). Similarly, we show here that
496 ncRNA had a positive effect on CD8+ T cell proliferation *in vitro* and *in vivo* in an
497 OVA model (Fig. 4) and was confirmed with the gp33-41 antigen model (Fig. 5).
498 Improvement of antigen cross-presentation by ncRNA could be explained by
499 modulation of antigen processing (16),(47),(48),(49). However, further experiments are
500 required to evaluate if enhanced co-stimulatory molecule expression and/or secreted
501 cytokine induced by ncRNA could alternatively explain the improvement of CD8+ T
502 cell activation.

503 ncRNA also modulates CD4+ T cell polarization. Indeed, we observed that ncRNA
504 promotes Th1 CD4+ responses rather than Th2 CD4+ responses, as (i) secretion by
505 BMDCs of TNF α is significantly increased, but not of IL-4, (ii) T-bet transcription
506 factor expression is slightly increased *in vivo* in activated CD4+ T cells while GATA3
507 expression is slightly decreased, and (iii) transcriptome studies revealed Th1
508 response-associated signatures. More specifically, upregulation of the *Irf1* gene,
509 which is involved in the regulation of interferon secretion and DC maturation
510 associated with Th1 polarization (50), was observed and confirmed by RT-qPCR. We
511 also showed in the presence of ncRNA a higher expression of the *Xcl1* gene, which
512 has been shown to be involved in antigen cross-presentation by DCs (51), and
513 upregulation of the *Slc2a6* gene that correlates with the magnitude of the antigen-
514 specific CD8+ T cell responses (52). These observations are therefore consistent with
515 the ability of ncRNA to improve CD8+ T cell proliferation and supported by others
516 demonstrating the role of TLR7/8 ligands in inducing Th1 responses (53),(54).
517 Altogether, we think ncRNA could be particularly favorable for HIV vaccine
518 development, since a Th2-biased CD4+ T cell response has been associated with
519 disease progression (54),(55), while Th1 responses have been shown to favor anti-
520 HIV-1 immunity (56). In the vaccination experiments, we observed that *ncRNA*VLPs
521 induce longer lasting humoral responses. We believe *ncRNA*VLPs are able to activate
522 more efficiently follicular helper T cells, leading to a better memory induction, as it

523 has already been shown with a TLR3 ligand encapsidated in HIV-derived VLPs (57).
524 This question is currently under investigation in our laboratory.

525 While VLPs and _{ncRNA}VLPs have similar levels of total packaged RNA, we
526 demonstrated here that ncRNA carried into _{ncRNA}VLPs has a unique TLR-dependent
527 adjuvant property in contrast to host RNAs. One remaining question concerns the
528 molecular pattern that confers its immunogenicity to ncRNA. Specific TLR7/8 ligand
529 motifs such as polyuridine sequences that would explain the induced MyD88-
530 signaling were not identified in the ncRNA sequence. Additional efforts should be
531 made in the near future to better characterize ncRNA-related immunogenicity and
532 establish a TLR7/8-dependent mechanism.

533 In conclusion, this study provides new evidence of MLV-derived VLP
534 immunogenicity, and demonstrates the advantages of using ncRNA as an
535 encapsulated adjuvant molecule. These observations warrant further evaluation in
536 prime-boost and/or in mucosal vaccine approaches, especially for HIV vaccination,
537 but also in allergen-specific immunotherapy with the specific aim of shifting the
538 immune response from the allergic Th2 to the non-allergic Th1 responses.

539

540 **Acknowledgments**

541 This work was supported by ANRS, UPMC and INSERM.

542 We thank the personnel of the Post-Genomic Platform (P3S) of the Pitié-Salpêtrière
543 Hospital in Paris for their involvement in the transcriptome experiments, and Omar
544 Chuquisana and Faustine Brimaud for their technical help.

545

546 **References**

- 547 1. Kushnir N, Streatfield SJ, Yusibov V. 2012. Virus-like particles as a highly efficient
548 vaccine platform: diversity of targets and production systems and advances in clinical
549 development. *Vaccine* 31:58–83.
- 550 2. Bachmann MF, Jennings GT. 2010. Vaccine delivery: a matter of size, geometry,
551 kinetics and molecular patterns. *Nat Rev Immunol* 10:787–796.
- 552 3. Noad R, Roy P. 2003. Virus-like particles as immunogens. *Trends Microbiol* 11:438–
553 444.
- 554 4. Chackerian B. 2007. Virus-like particles: flexible platforms for vaccine development.
555 *Expert Rev Vaccines* 6:381–390.
- 556 5. Campo JJ, Sacarlal J, Aponte JJ, Aide P, Nhabomba AJ, Dobaño C, Alonso PL. 2014.
557 Duration of vaccine efficacy against malaria: 5th year of follow-up in children vaccinated
558 with RTS,S/AS02 in Mozambique. *Vaccine* 32:2209–2216.
- 559 6. Garrone P, Fluckiger A-C, Mangeot PE, Gauthier E, Dupeyrot-Lacas P, Mancip J,
560 Cangialosi A, Du Chéné I, LeGrand R, Mangeot I, Lavillette D, Bellier B, Cosset F-L,
561 Tangy F, Klatzmann D, Dalba C. 2011. A prime-boost strategy using virus-like particles
562 pseudotyped for HCV proteins triggers broadly neutralizing antibodies in macaques. *Sci*
563 *Transl Med* 3:94ra71.
- 564 7. Bellier B, Dalba C, Clerc B, Desjardins D, Drury R, Cosset F-L, Collins M, Klatzmann D.
565 2006. DNA vaccines encoding retrovirus-based virus-like particles induce efficient
566 immune responses without adjuvant. *Vaccine* 24:2643–2655.
- 567 8. Bellier B, Huret C, Miyalou M, Desjardins D, Frenkiel M-P, Despres P, Tangy F, Dalba
568 C, Klatzmann D. 2009. DNA vaccines expressing retrovirus-like particles are efficient
569 immunogens to induce neutralizing antibodies. *Vaccine* 27:5772–5780.

- 570 9. Huret C, Desjardins D, Miyalou M, Levacher B, Amadoudji Zin M, Bonduelle O,
571 Combadière B, Dalba C, Klatzmann D, Bellier B. 2013. Recombinant retrovirus-derived
572 virus-like particle-based vaccines induce hepatitis C virus-specific cellular and
573 neutralizing immune responses in mice. *Vaccine* 31:1540–1547.
- 574 10. Lescaille G, Pitoiset F, Macedo R, Baillou C, Huret C, Klatzmann D, Tartour E, Lemoine
575 FM, Bellier B. 2013. Efficacy of DNA vaccines forming e7 recombinant retroviral virus-
576 like particles for the treatment of human papillomavirus-induced cancers. *Hum Gene*
577 *Ther* 24:533–544.
- 578 11. Sindhu S, Toma E, Cordeiro P, Ahmad R, Morisset R, Menezes J. 2006. Relationship of
579 in vivo and ex vivo levels of TH1 and TH2 cytokines with viremia in HAART patients
580 with and without opportunistic infections. *J Med Virol* 78:431–439.
- 581 12. García-Díaz D, Rodríguez I, Santisteban Y, Márquez G, Terrero Y, Brown E, Iglesias E.
582 2013. Th2-Th1 shift with the multiantigenic formulation TERA-VAC-HIV-1 in Balb/c mice.
583 *Immunol Lett* 149:77–84.
- 584 13. Olive C. 2012. Pattern recognition receptors: sentinels in innate immunity and targets of
585 new vaccine adjuvants. *Expert Rev Vaccines* 11:237–256.
- 586 14. Steinhagen F, Kinjo T, Bode C, Klinman DM. 2011. TLR-based immune adjuvants.
587 *Vaccine* 29:3341–3355.
- 588 15. Beutler BA. 2009. TLRs and innate immunity. *Blood* 113:1399–1407.
- 589 16. Crespo MI, Zacca ER, Núñez NG, Ranocchia RP, Maccioni M, Maletto BA, Pistoresi-
590 Palencia MC, Morón G. 2013. TLR7 Triggering with Polyuridylic Acid Promotes Cross-
591 Presentation in CD8 α + Conventional Dendritic Cells by Enhancing Antigen Preservation
592 and MHC Class I Antigen Permanence on the Dendritic Cell Surface. *J Immunol*
593 190:948–960.

- 594 17. Fehres CM, Bruijns SCM, van Beelen AJ, Kalay H, Ambrosini M, Hooijberg E, Unger
595 WWJ, de Gruijl TD, van Kooyk Y. 2014. Topical rather than intradermal application of
596 the TLR7 ligand imiquimod leads to human dermal dendritic cell maturation and CD8(+)
597 T-cell cross-priming. *Eur J Immunol*.
- 598 18. Shirota H, Klinman DM. 2014. TLR-9 agonist immunostimulatory sequence adjuvants
599 linked to cancer antigens. *Methods Mol Biol Clifton NJ* 1139:337–344.
- 600 19. Soong R-S, Song L, Trieu J, Knoff J, He L, Tsai YC, Huh W, Chang Y-N, Cheng W-F,
601 Roden RBS, Wu T-C, Hung C-F. 2014. Toll like receptor agonist imiquimod facilitates
602 antigen-specific CD8+ T cell accumulation in the genital tract leading to tumor control
603 through interferon- γ . *Clin Cancer Res clincanres.0344.2014*.
- 604 20. Vasilakos JP, Tomai MA. 2013. The use of Toll-like receptor 7/8 agonists as vaccine
605 adjuvants. *Expert Rev Vaccines* 12:809–819.
- 606 21. Adachi O, Kawai T, Takeda K, Matsumoto M, Tsutsui H, Sakagami M, Nakanishi K,
607 Akira S. 1998. Targeted disruption of the MyD88 gene results in loss of IL-1- and IL-18-
608 mediated function. *Immunity* 9:143–150.
- 609 22. Yee JK, Friedmann T, Burns JC. 1994. Generation of high-titer pseudotyped retroviral
610 vectors with very broad host range. *Methods Cell Biol* 43 Pt A:99–112.
- 611 23. Shannon P, Markiel A, Ozier O, Baliga NS, Wang JT, Ramage D, Amin N, Schwikowski
612 B, Ideker T. 2003. Cytoscape: a software environment for integrated models of
613 biomolecular interaction networks. *Genome Res* 13:2498–2504.
- 614 24. Merico D, Isserlin R, Bader GD. 2011. Visualizing gene-set enrichment results using the
615 Cytoscape plug-in enrichment map. *Methods Mol Biol Clifton NJ* 781:257–277.

- 616 25. Margine I, Martinez-Gil L, Chou Y-Y, Krammer F. 2012. Residual baculovirus in insect
617 cell-derived influenza virus-like particle preparations enhances immunogenicity. *PloS*
618 *One* 7:e51559.
- 619 26. Soares HR, Castro R, Tomás HA, Rodrigues AF, Gomes-Alves P, Bellier B, Klatzmann
620 D, Carrondo MJT, Alves PM, Coroadinha AS. 2016. Tetraspanins displayed in
621 retrovirus-derived virus-like particles and their immunogenicity. *Vaccine* 34:1634–1641.
- 622 27. Moffat JM, Cheong W-S, Villadangos JA, Minter JD, Netter HJ. 2013. Hepatitis B virus-
623 like particles access major histocompatibility class I and II antigen presentation
624 pathways in primary dendritic cells. *Vaccine* 31:2310–2316.
- 625 28. Barth H, Ulsenheimer A, Pape GR, Diepolder HM, Hoffmann M, Neumann-Haefelin C,
626 Thimme R, Henneke P, Klein R, Paranhos-Baccalà G, Depla E, Liang TJ, Blum HE,
627 Baumert TF. 2005. Uptake and presentation of hepatitis C virus-like particles by human
628 dendritic cells. *Blood* 105:3605–3614.
- 629 29. Onafuwa-Nuga AA, King SR, Telesnitsky A. 2005. Nonrandom packaging of host RNAs
630 in moloney murine leukemia virus. *J Virol* 79:13528–13537.
- 631 30. Rulli SJ, Hibbert CS, Mirro J, Pederson T, Biswal S, Rein A. 2007. Selective and
632 nonselective packaging of cellular RNAs in retrovirus particles. *J Virol* 81:6623–6631.
- 633 31. Fife KH, Meng T-C, Ferris DG, Liu P. 2008. Effect of Resiquimod 0.01% Gel on Lesion
634 Healing and Viral Shedding When Applied to Genital Herpes Lesions. *Antimicrob*
635 *Agents Chemother* 52:477–482.
- 636 32. Wu CCN, Hayashi T, Takabayashi K, Sabet M, Smee DF, Guiney DD, Cottam HB,
637 Carson DA. 2007. Immunotherapeutic activity of a conjugate of a Toll-like receptor 7
638 ligand. *Proc Natl Acad Sci U S A* 104:3990–3995.

- 639 33. Wille-Reece U, Flynn BJ, Loré K, Koup RA, Kedl RM, Mattapallil JJ, Weiss WR,
640 Roederer M, Seder RA. 2005. HIV Gag protein conjugated to a Toll-like receptor 7/8
641 agonist improves the magnitude and quality of Th1 and CD8+ T cell responses in
642 nonhuman primates. *Proc Natl Acad Sci U S A* 102:15190–15194.
- 643 34. Moody MA, Santra S, Vandergrift NA, Sutherland LL, Gurley TC, Drinker MS, Allen AA,
644 Xia S-M, Meyerhoff RR, Parks R, Lloyd KE, Easterhoff D, Alam SM, Liao H-X, Ward
645 BM, Ferrari G, Montefiori DC, Tomaras GD, Seder RA, Letvin NL, Haynes BF. 2014.
646 Toll-like receptor 7/8 (TLR7/8) and TLR9 agonists cooperate to enhance HIV-1
647 envelope antibody responses in rhesus macaques. *J Virol* 88:3329–3339.
- 648 35. Gibson SJ, Lindh JM, Riter TR, Gleason RM, Rogers LM, Fuller AE, Oesterich JL,
649 Gorden KB, Qiu X, McKane SW, Noelle RJ, Miller RL, Kedl RM, Fitzgerald-Bocarsly P,
650 Tomai MA, Vasilakos JP. 2002. Plasmacytoid dendritic cells produce cytokines and
651 mature in response to the TLR7 agonists, imiquimod and resiquimod. *Cell Immunol*
652 218:74–86.
- 653 36. Ahonen CL, Gibson SJ, Smith RM, Pederson LK, Lindh JM, Tomai MA, Vasilakos JP.
654 1999. Dendritic cell maturation and subsequent enhanced T-cell stimulation induced
655 with the novel synthetic immune response modifier R-848. *Cell Immunol* 197:62–72.
- 656 37. Hemmi H, Kaisho T, Takeuchi O, Sato S, Sanjo H, Hoshino K, Horiuchi T, Tomizawa H,
657 Takeda K, Akira S. 2002. Small anti-viral compounds activate immune cells via the
658 TLR7 MyD88-dependent signaling pathway. *Nat Immunol* 3:196–200.
- 659 38. Saitoh T, Satoh T, Yamamoto N, Uematsu S, Takeuchi O, Kawai T, Akira S. 2011.
660 Antiviral protein Viperin promotes Toll-like receptor 7- and Toll-like receptor 9-mediated
661 type I interferon production in plasmacytoid dendritic cells. *Immunity* 34:352–363.

- 662 39. Lombardi V, Van Overtvelt L, Horiot S, Moingeon P. 2009. Human dendritic cells
663 stimulated via TLR7 and/or TLR8 induce the sequential production of Il-10, IFN-gamma,
664 and IL-17A by naive CD4+ T cells. *J Immunol Baltim Md 1950* 182:3372–3379.
- 665 40. Querec TD, Akondy RS, Lee EK, Cao W, Nakaya HI, Teuwen D, Pirani A, Gernert K,
666 Deng J, Marzolf B, Kennedy K, Wu H, Bennouna S, Oluoch H, Miller J, Vencio RZ,
667 Mulligan M, Aderem A, Ahmed R, Pulendran B. 2009. Systems biology approach
668 predicts immunogenicity of the yellow fever vaccine in humans. *Nat Immunol* 10:116–
669 125.
- 670 41. Gaucher D, Therrien R, Kettaf N, Angermann BR, Boucher G, Filali-Mouhim A, Moser
671 JM, Mehta RS, Drake DR, Castro E, Akondy R, Rinfret A, Yassine-Diab B, Said EA,
672 Chouikh Y, Cameron MJ, Clum R, Kelvin D, Somogyi R, Greller LD, Balderas RS,
673 Wilkinson P, Pantaleo G, Tartaglia J, Haddad EK, Sékaly R-P. 2008. Yellow fever
674 vaccine induces integrated multilineage and polyfunctional immune responses. *J Exp*
675 *Med* 205:3119–3131.
- 676 42. Nakaya HI, Wrammert J, Lee EK, Racioppi L, Marie-Kunze S, Haining WN, Means AR,
677 Kasturi SP, Khan N, Li G-M, McCausland M, Kanchan V, Kokko KE, Li S, Elbein R,
678 Mehta AK, Aderem A, Subbarao K, Ahmed R, Pulendran B. 2011. Systems biology of
679 vaccination for seasonal influenza in humans. *Nat Immunol* 12:786–795.
- 680 43. Li S, Roupheal N, Duraisingham S, Romero-Steiner S, Presnell S, Davis C, Schmidt
681 DS, Johnson SE, Milton A, Rajam G, Kasturi S, Carlone GM, Quinn C, Chaussabel D,
682 Palucka AK, Mulligan MJ, Ahmed R, Stephens DS, Nakaya HI, Pulendran B. 2014.
683 Molecular signatures of antibody responses derived from a systems biology study of
684 five human vaccines. *Nat Immunol* 15:195–204.
- 685 44. Wysocka M, Newton S, Benoit BM, Introcaso C, Hancock AS, Chehimi J, Richardson
686 SK, Gelfand JM, Montaner LJ, Rook AH. 2007. Synthetic imidazoquinolines potently

- 687 and broadly activate the cellular immune response of patients with cutaneous T-cell
688 lymphoma: synergy with interferon-gamma enhances production of interleukin-12. *Clin*
689 *Lymphoma Myeloma* 7:524–534.
- 690 45. Lebel M-È, Daudelin J-F, Chartrand K, Tarrab E, Kalinke U, Savard P, Labrecque N,
691 Leclerc D, Lamarre A. 2014. Nanoparticle adjuvant sensing by TLR7 enhances CD8+ T
692 cell-mediated protection from *Listeria monocytogenes* infection. *J Immunol Baltim Md*
693 1950 192:1071–1078.
- 694 46. Wille-Reece U, Wu C, Flynn BJ, Kedi RM, Seder RA. 2005. Immunization with HIV-1
695 Gag Protein Conjugated to a TLR7/8 Agonist Results in the Generation of HIV-1 Gag-
696 Specific Th1 and CD8+ T Cell Responses. *J Immunol* 174:7676–7683.
- 697 47. Oh JZ, Kurche JS, Burchill MA, Kedi RM. 2011. TLR7 enables cross-presentation by
698 multiple dendritic cell subsets through a type I IFN-dependent pathway. *Blood*
699 118:3028–3038.
- 700 48. Stephenson RM, Lim CM, Matthews M, Dietsch G, Hershberg R, Ferris RL. 2013. TLR8
701 stimulation enhances cetuximab-mediated natural killer cell lysis of head and neck
702 cancer cells and dendritic cell cross-priming of EGFR-specific CD8+ T cells. *Cancer*
703 *Immunol Immunother CII* 62:1347–1357.
- 704 49. Oh JZ, Kedi RM. 2010. The capacity to induce cross-presentation dictates the success
705 of a TLR7 agonist-conjugate vaccine for eliciting cellular immunity. *J Immunol Baltim Md*
706 1950 185:4602–4608.
- 707 50. Castaldello A, Sgarbanti M, Marsili G, Brocca-Cofano E, Remoli AL, Caputo A, Battistini
708 A. 2010. Interferon regulatory factor-1 acts as a powerful adjuvant in tat DNA based
709 vaccination. *J Cell Physiol* 224:702–709.

- 710 51. Kroczek RA, Henn V. 2012. The Role of XCR1 and its Ligand XCL1 in Antigen Cross-
711 Presentation by Murine and Human Dendritic Cells. *Front Immunol* 3:14.
- 712 52. Buonaguro L, Wang E, Tornesello ML, Buonaguro FM, Marincola FM. 2011. Systems
713 biology applied to vaccine and immunotherapy development. *BMC Syst Biol* 5:146.
- 714 53. Wagner TL, Ahonen CL, Couture AM, Gibson SJ, Miller RL, Smith RM, Reiter MJ,
715 Vasilakos JP, Tomai MA. 1999. Modulation of TH1 and TH2 cytokine production with
716 the immune response modifiers, R-848 and imiquimod. *Cell Immunol* 191:10–19.
- 717 54. Chang BA, Cross JL, Najjar HM, Dutz JP. 2009. Topical resiquimod promotes priming of
718 CTL to parenteral antigens. *Vaccine* 27:5791–5799.
- 719 55. Wang J, Harada A, Matsushita S, Matsumi S, Zhang Y, Shioda T, Nagai Y, Matsushima
720 K. 1998. IL-4 and a glucocorticoid up-regulate CXCR4 expression on human CD4+ T
721 lymphocytes and enhance HIV-1 replication. *J Leukoc Biol* 64:642–649.
- 722 56. Pleguezuelos O, Stoloff GA, Caparrós-Wanderley W. 2013. Synthetic immunotherapy
723 induces HIV virus specific Th1 cytotoxic response and death of an HIV-1 infected
724 human cell line through classic complement activation. *Virol J* 10:107.
- 725 57. Poteet E, Lewis P, Chen C, Ho SO, Do T, Chiang S, Labranche C, Montefiori D, Fujii G,
726 Yao Q. 2016. Toll-like receptor 3 adjuvant in combination with virus-like particles elicit a
727 humoral response against HIV. *Vaccine* 34:5886–5894.

728

729 **Figure legends**

730 **Figure 1**

731 **ncRNA system and validation of $_{ncRNA}$ VLPs. (A)** Structure of the ncRNA encoding
732 plasmid. Box sizes indicates the relative length of the genetic sequences according
733 to the scale provided. CMV: cytomegalovirus immediate-early promoter; psi: retroviral
734 encapsidation sequence; U3, R, U5: MLV-long terminal repeat (LTR) sequences. **(B)**
735 Schematic representation of MLV-derived standard VLPs (left) and $_{ncRNA}$ VLPs (right).
736 Packaged cellular RNAs and ncRNA (two copies of single-stranded virus-derived
737 RNA) are illustrated. **(C)** Validation by RT-qPCR of the presence of ncRNA in the
738 pseudo-particles. Gray curves: VLPs; black curves: $_{ncRNA}$ VLPs. Untransfected cell
739 lysate was used as negative control (dashed curves). Duplicates of one experiment
740 representative of three are shown. **(D)** ncRNA-specific qPCR conducted on VLPs or
741 $_{ncRNA}$ VLPs, with (plain curves) or without (dashed curves) reverse transcriptase step.
742 **(E)** Evaluation of endotoxin levels in three different production batches of VLPs and
743 $_{ncRNA}$ VLPs using LAL assay. Commercial OVA protein batch was used as control.

744 **Figure 2**

745 ***In vitro* effect of VLPs carrying or not ncRNA on bone marrow-derived**
746 **dendritic cell activation.** Immature BMDCs from C57BL/6 **(A-F)** or MyD88^{-/-} **(G-L)**
747 mice were incubated for 24 hours in the presence of 1, 5 or 10 µg/mL of VSV-G
748 pseudotyped MLV-Gag VLPs or $_{ncRNA}$ VLPs. CD80 and CD86 expressions were
749 analyzed by flow cytometry. Representative histograms of CD80 **(A, G)** and CD86 **(B,**
750 **H)** on C57BL/6 BMDCs **(A-B)** or MyD88^{-/-} BMDCs **(G-H)** cultured with 5 µg/mL of
751 VLPs (thin line), $_{ncRNA}$ VLPs (thick line) or medium alone (plain histogram) are shown.
752 Related percentages of CD80+ **(C, I)** and CD86+ **(D, J)** were represented. Medium
753 alone, LPS (100 ng/mL) and R848 (1 µg/mL) were used as negative control and two
754 positive controls, respectively. Results represent the mean + SD of duplicates for
755 each dose of VLPs from one experiment representative of two **(C-D, I-J)** and the
756 means +/- SEM of two independent experiments with the dose of 5 µg/mL are
757 represented for CD80 **(E, K)** and CD86 **(F, L)** for C57BL/6 **(E, F)** and MyD88^{-/-} **(K, L)**
758 BMDCs. * p ≤ 0.05, ns: not significant; Mann-Whitney test.

759 **Figure 3**

760 **Transcriptome analysis of splenic dendritic cells after *in vivo* injection of VLPs**
761 **or ncRNA VLPs.** Dendritic-specific gene set enrichment analysis using Gene Ontology
762 database signatures allowed us to identify molecular signatures that are differentially
763 enriched in VLP and ncRNA VLP groups compared with PBS. **(A)** Results were mapped
764 using Cytoscape software as a network of signatures (nodes) related by similarity
765 (edges). Node size is proportional to the total number of genes in each set. Groups of
766 functionally related signatures are circled and labeled (modules). Grey nodes
767 represent signatures shared between VLP and ncRNA VLP groups; red nodes represent
768 signatures that are specific for the ncRNA VLP group. FDR q-value = 0.05, P-value =
769 0.005. **(B)** Heatmap showing three ncRNA-specific signatures. Samples were
770 clustered using a distance-based hierarchical clustering regarding the gene
771 expression. The heatmap colors represent the gene expression (red for high, black
772 for middle, and green for low expression). The Gene Ontology exact names of
773 signatures are “Dendritic cell differentiation” for DC differentiation, “Positive
774 regulation of Toll-Like receptor signaling pathways” for TLR signaling, and “Positive
775 regulation of T helper type 1 immune response” for Th1 response. **(C)** Validation by
776 RT-qPCR of the relative quantity of eight different genes from the three selected
777 signatures.

778 **Figure 4**

779 ***In vitro* and *in vivo* effects of VLPs carrying or not ncRNA on T cell proliferation**
780 **and polarization. (A, B)** *In vitro* proliferation of antigen-specific CD8⁺ T cells. CFSE-
781 stained OVA-specific OT-I splenic lymphocytes were cultured for 3 days with antigen-
782 presenting cells from C57BL/6 **(A)** or MyD88^{-/-} **(B)** in the presence of 5 µg/mL of VSV-
783 G pseudotyped Gag-OVA VLPs (gray bars) or ncRNA VLPs (black bars). Percentages
784 of divided cells were evaluated by flow cytometry analysis of CFSE-low cells among
785 CD8⁺ Vα2⁺ live cells. Medium alone and OVA-I peptide were used as negative and
786 positive controls, respectively. Means of triplicates from three independent
787 experiments are shown. **(C-E)** *In vivo* proliferation of antigen-specific CD8⁺ T cells.
788 C57BL/6 or MyD88^{-/-} mice (n = 5 per group) were injected i.v. with 1 µg of VSV-G
789 pseudotyped Gag-OVA VLPs or ncRNA VLPs, and PBS in the control group. Six hours
790 later mice received 1.5x10⁶ CFSE⁺ OVA-specific CD8⁺ T cells from OT-I mice. After
791 3 days, spleens were collected and proliferation of OVA-specific CD8⁺ T cells was
792 evaluated by flow cytometry. One representative dot plot of the CFSE profile from

793 each group is depicted in **(C)**. Percentages of divided OVA-specific CD8⁺ T cells for
794 each dose in C57BL/6 **(D)** and MyD88^{-/-} mice **(E)** are shown. Results represent the
795 mean values +SEM. **(F, G)** *In vivo* proliferation and differentiation of antigen-specific
796 CD4⁺ T cells. The same experiment as in **(D)** was conducted with OT-II cells instead
797 of OT-I cells. **(F)** Means of the percentage of divided OVA-specific CD4⁺ T cells and
798 SEM are shown. Geometric means (MFI) ratios of Tbet : GATA3 expression among
799 divided CD4⁺ T cells are represented in **(G)**. * p ≤ 0.05, ** p ≤ 0.01, ns: not significant;
800 Mann-Whitney test.

801 **Figure 5:**

802 **T- and B-cell immune responses in mice vaccinated with HIV-pseudotyped**
803 **VLPs carrying or not ncRNA. (A)** Schematic representation of the vaccination
804 protocol. C57BL/6 or MyD88^{-/-} mice (n = 5 per group) were immunized 3 times at
805 two-week intervals with 25 µg of HIV-pseudotyped Gag-gp33-41 VLPs or ncRNA VLPs.
806 Sera were collected from blood samples at weeks 6 and 12. **(B, C)** Cellular
807 responses were evaluated at week 12 by standard IFN-γ ELISPOT after specific
808 restimulation with either gp33-41 **(B)** or HIV-gp140 **(C)**. Results represent individual
809 values and group means expressed as number of spot forming units (SFUs) per
810 million of splenocytes. **(D, E)** Specific anti-gp140 antibody concentrations were
811 evaluated in serum of immunized or naïve C57BL/6 mice by anti-GP120 ELISA at
812 weeks 6 **(D)** and 12 **(E)**. Results represent the mean values + SEM of measured
813 concentrations. * p ≤ 0.05, ** p ≤ 0.01; Mann-Whitney test.

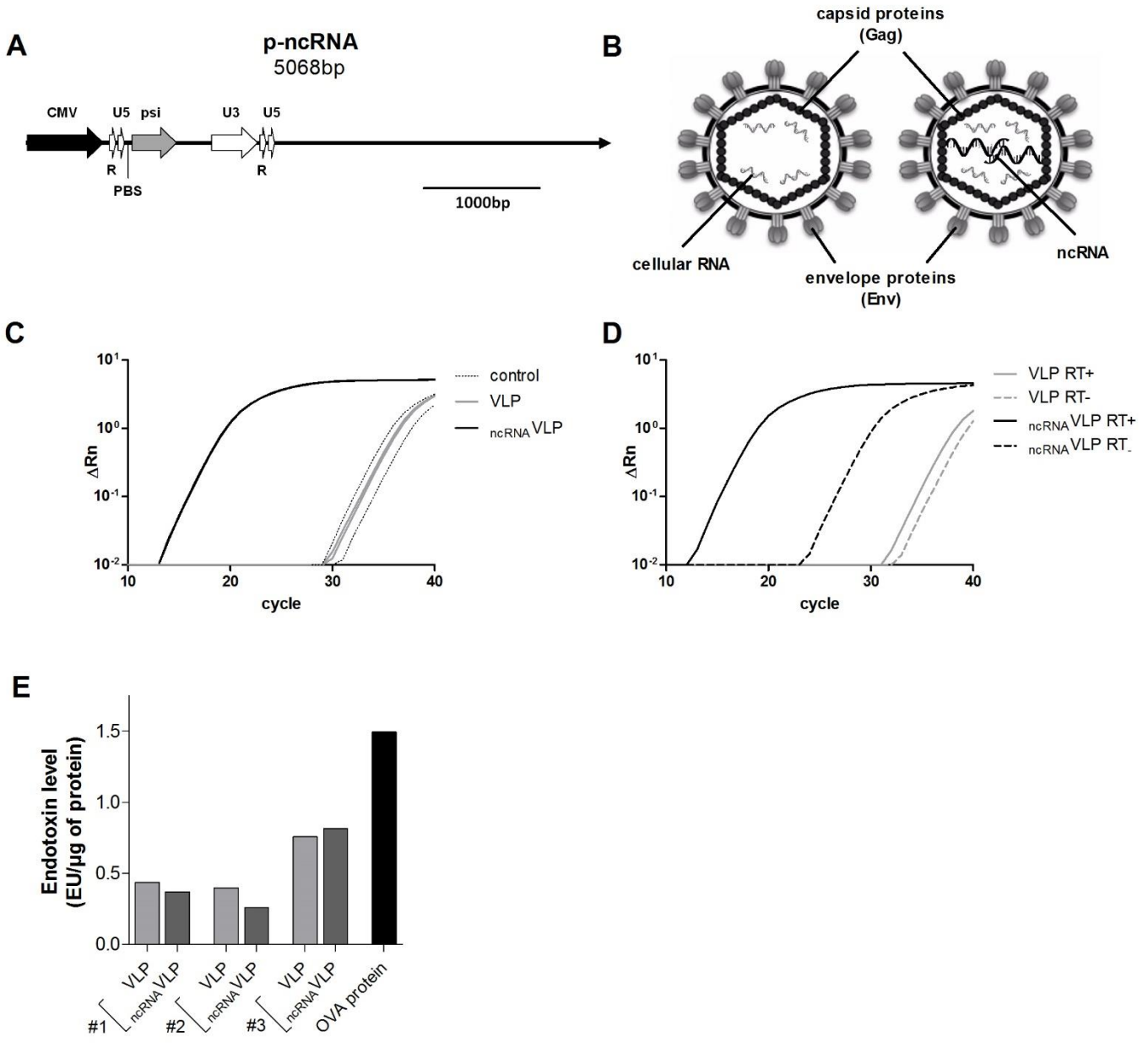


Figure 1:

ncRNA system and validation of $ncRNA$ VLPs. **(A)** Structure of the ncRNA encoding plasmid. Box sizes indicate the relative length of the genetic sequences according to the scale provided. CMV: cytomegalovirus immediate-early promoter; psi: retroviral encapsidation sequence; U3, R, U5: MLV-long terminal repeat (LTR) sequences. **(B)** Schematic representation of MLV-derived standard VLPs (left) and $ncRNA$ VLPs (right). Packaged cellular RNAs and ncRNA (two copies of single-stranded virus-derived RNA) are illustrated. **(C)** Validation by RT-qPCR of the presence of ncRNA in the pseudo-particles. Gray curves: VLPs; black curves: $ncRNA$ VLPs. Untransfected cell lysate was used as negative control (dashed curves). Duplicates of one experiment representative of three are shown. **(D)** ncRNA-specific qPCR conducted on VLPs or $ncRNA$ VLPs, with (plain curves) or without (dashed curves) reverse transcriptase step. **(E)** Evaluation of endotoxin levels in three different production batches of VLPs and $ncRNA$ VLPs using LAL assay. Commercial OVA protein batch was used as control.

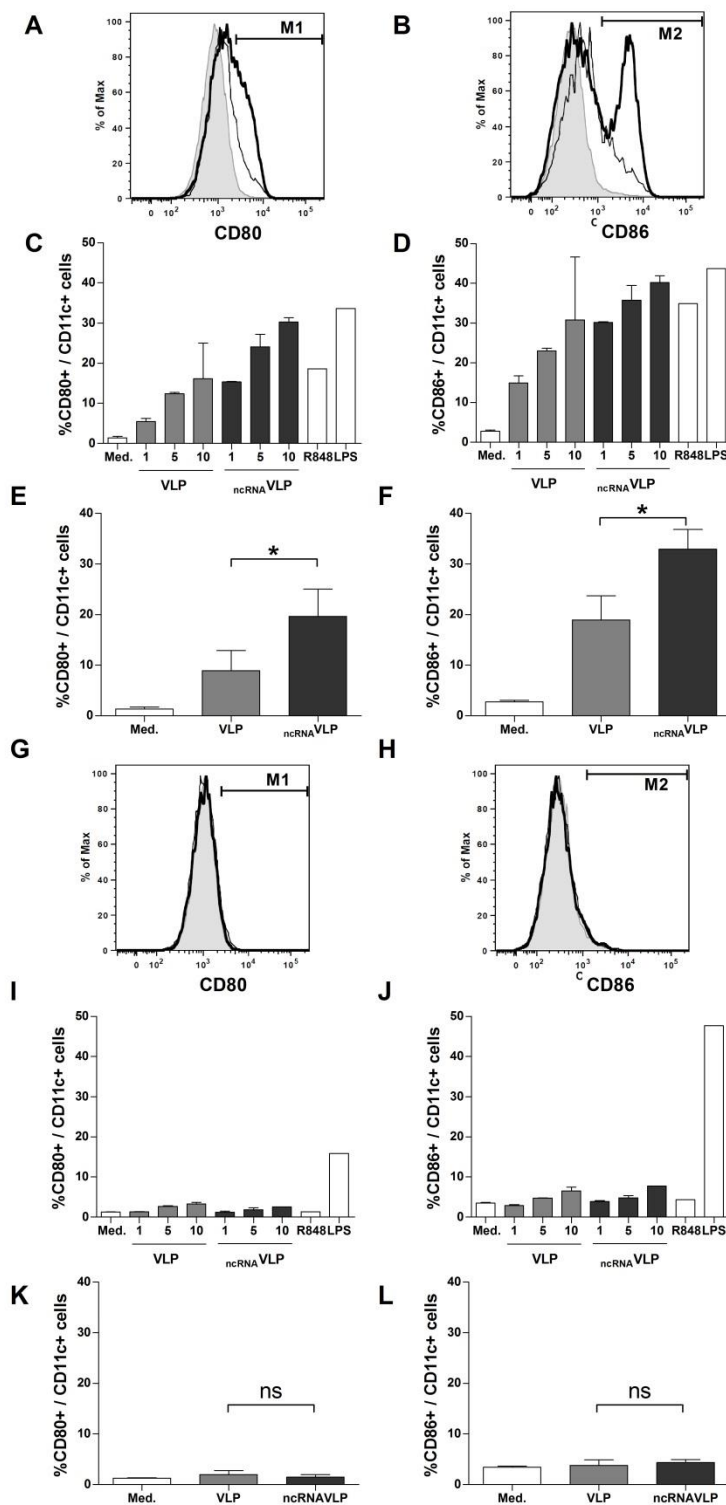


Figure 2:

***In vitro* effect of VLPs carrying or not ncRNA on bone marrow-derived dendritic cell activation.** Immature BMDCs from C57BL/6 (A-F) or MyD88^{-/-} (G-L) mice were incubated for 24 hours in the presence of 1, 5 or 10 µg/mL of VSV-G pseudotyped MLV-Gag VLPs or ncRNA VLPs. CD80 and CD86 expressions were analyzed by flow cytometry. Representative histograms of CD80 (A, G) and CD86 (B, H) on C57BL/6 BMDCs (A-B) or MyD88^{-/-} BMDCs (G-H) cultured with 5 µg/mL of VLPs (thin line), ncRNA VLPs (thick line) or medium alone (plain histogram) are shown. Related percentages of CD80+ (C, I) and CD86+ (D, J) were represented. Medium alone, LPS (100 ng/mL) and R848 (1 µg/mL) were used as negative control and two positive controls, respectively. Results represent the mean + SD of duplicates for each dose of VLPs from one experiment representative of two (C-D, I-J) and the means +/- SEM of two independent experiments with the dose of 5 µg/mL are represented for CD80 (E, K) and CD86 (F, L) for C57BL/6 (E, F) and MyD88^{-/-} (K, L) BMDCs. * p < 0.05, ns: not significant; Mann-Whitney test.

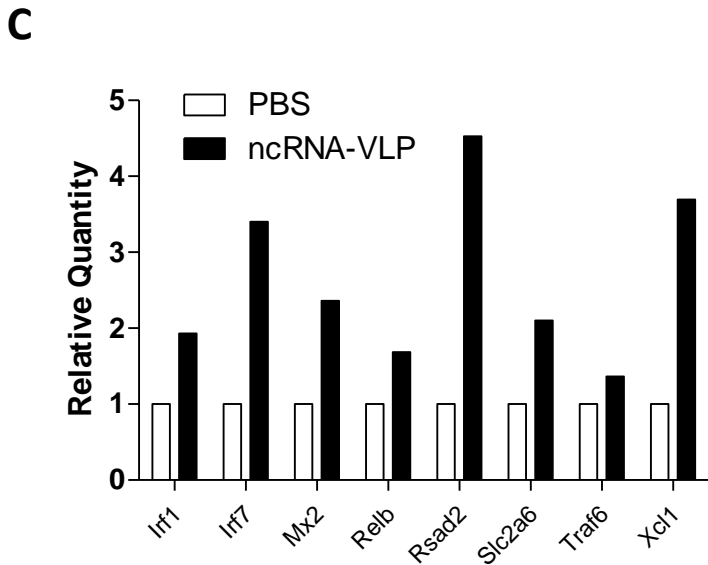
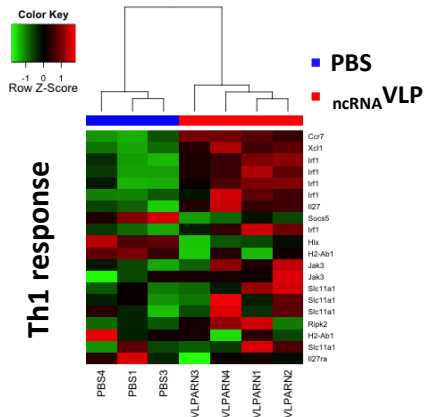
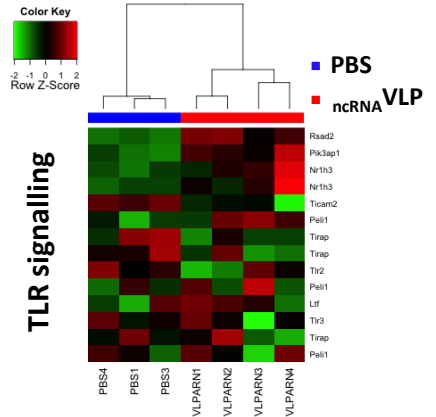
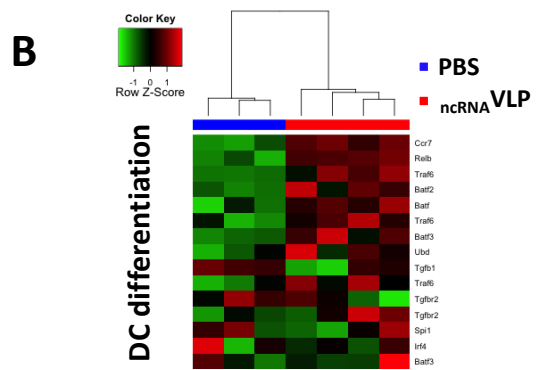
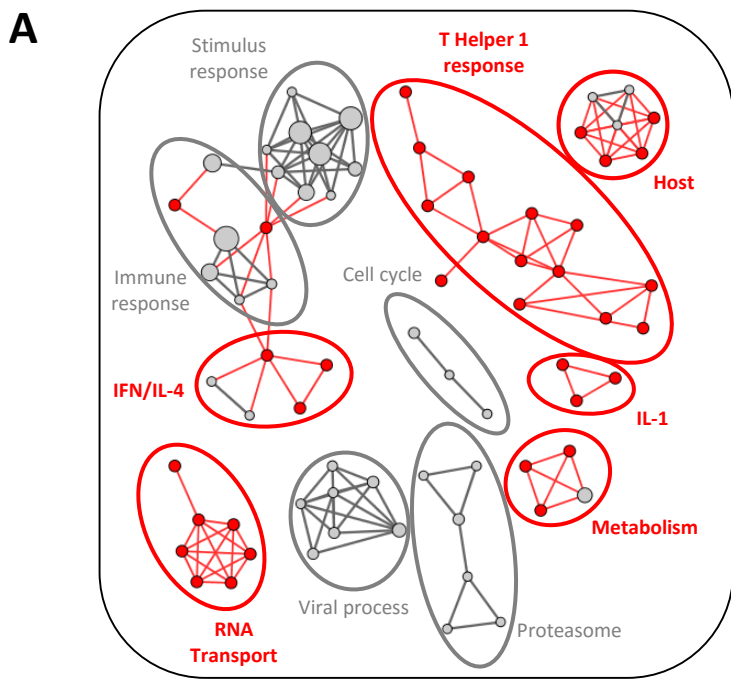


Figure 3:

Transcriptome analysis of splenic dendritic cells after *in vivo* injection of VLPs or ncRNA VLPs. Dendritic-specific gene set enrichment analysis using Gene Ontology database signatures allowed us to identify molecular signatures that are differentially enriched in VLP and ncRNA VLP groups compared with PBS. **(A)** Results were mapped using Cytoscape software as a network of signatures (nodes) related by similarity (edges). Node size is proportional to the total number of genes in each set. Groups of functionally related signatures are circled and labeled (modules). Grey nodes represent signatures shared between VLP and ncRNA VLP groups; red nodes represent signatures that are specific for the ncRNA VLP group. FDR q-value = 0.05, P-value = 0.005. **(B)** Heatmap showing three ncRNA-specific signatures. Samples were clustered using a distance-based hierarchical clustering regarding the gene expression. The heatmap colors represent the gene expression (red for high, black for middle, and green for low expression). The Gene Ontology exact names of signatures are “Dendritic cell differentiation” for DC differentiation, “Positive regulation of Toll-Like receptor signaling pathways” for TLR signaling, and “Positive regulation of T helper type 1 immune response” for Th1 response. **(C)** Validation by RT-qPCR of the relative quantity of eight different genes from the three selected signatures.

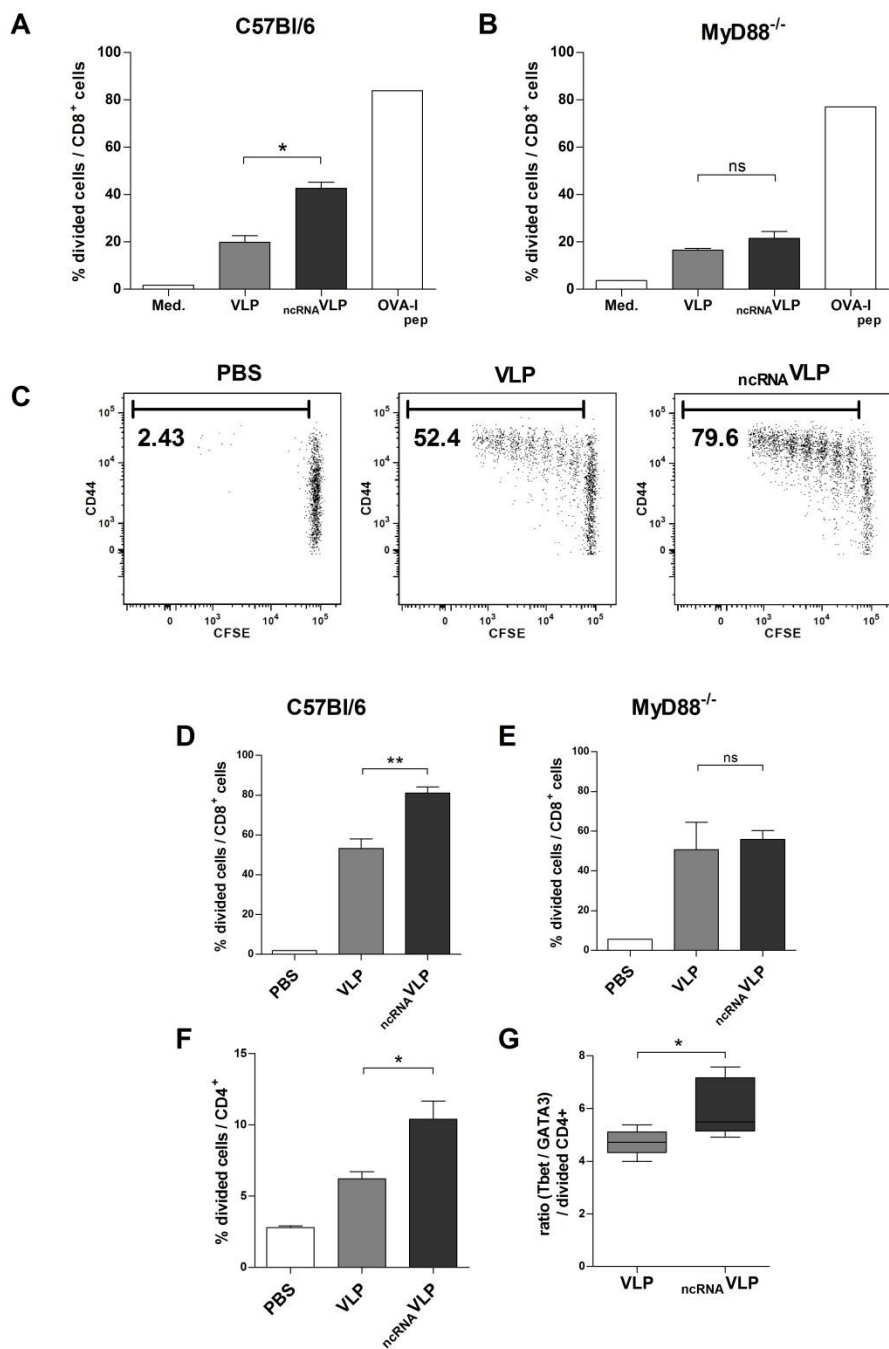


Figure 4:

***In vitro* and *in vivo* effects of VLPs carrying or not ncRNA on T cell proliferation and polarization. (A, B)** *In vitro* proliferation of antigen-specific CD8⁺ T cells. CFSE-stained OVA-specific OT-I splenic lymphocytes were cultured for 3 days with antigen-presenting cells from C57BL/6 (A) or MyD88^{-/-} (B) in the presence of 5 μg/mL of VSV-G pseudotyped Gag-OVA VLPs (gray bars) or ncRNA VLPs (black bars). Percentages of divided cells were evaluated by flow cytometry analysis of CFSE-low cells among CD8⁺ Vα2⁺ live cells. Medium alone and OVA-I peptide were used as negative and positive controls, respectively. Means of triplicates from three independent experiments are shown. (C-E) *In vivo* proliferation of antigen-specific CD8⁺ T cells. C57BL/6 or MyD88^{-/-} mice (n = 5 per group) were injected i.v. with 1 μg of VSV-G pseudotyped Gag-OVA VLPs or ncRNA VLPs, and PBS in the control group. Six hours later received 1.5x10⁶ CFSE⁺ OVA-specific CD8⁺ T cells from OT-I mice. After 3 days, spleens were collected and proliferation of OVA-specific CD8⁺ T cells was evaluated by flow cytometry. One representative dot plot of the CFSE profile from each group is depicted in (C). Percentages of divided OVA-specific CD8⁺ T cells for each dose in C57BL/6 (D) and MyD88^{-/-} mice (E) are shown. Results represent the mean values +SEM. (F, G) *In vivo* proliferation and differentiation of antigen-specific CD4⁺ T cells. The same experiment as in (D) was conducted with OT-II cells instead of OT-I cells. (F) Means of the percentage of divided OVA-specific CD4⁺ T cells and SEM are shown. Geometric means (MFI) ratios of Tbet : GATA3 expression among divided CD4⁺ T cells are represented in (G). * p < 0.05, ** p < 0.01, ns: not significant; Mann-Whitney test.

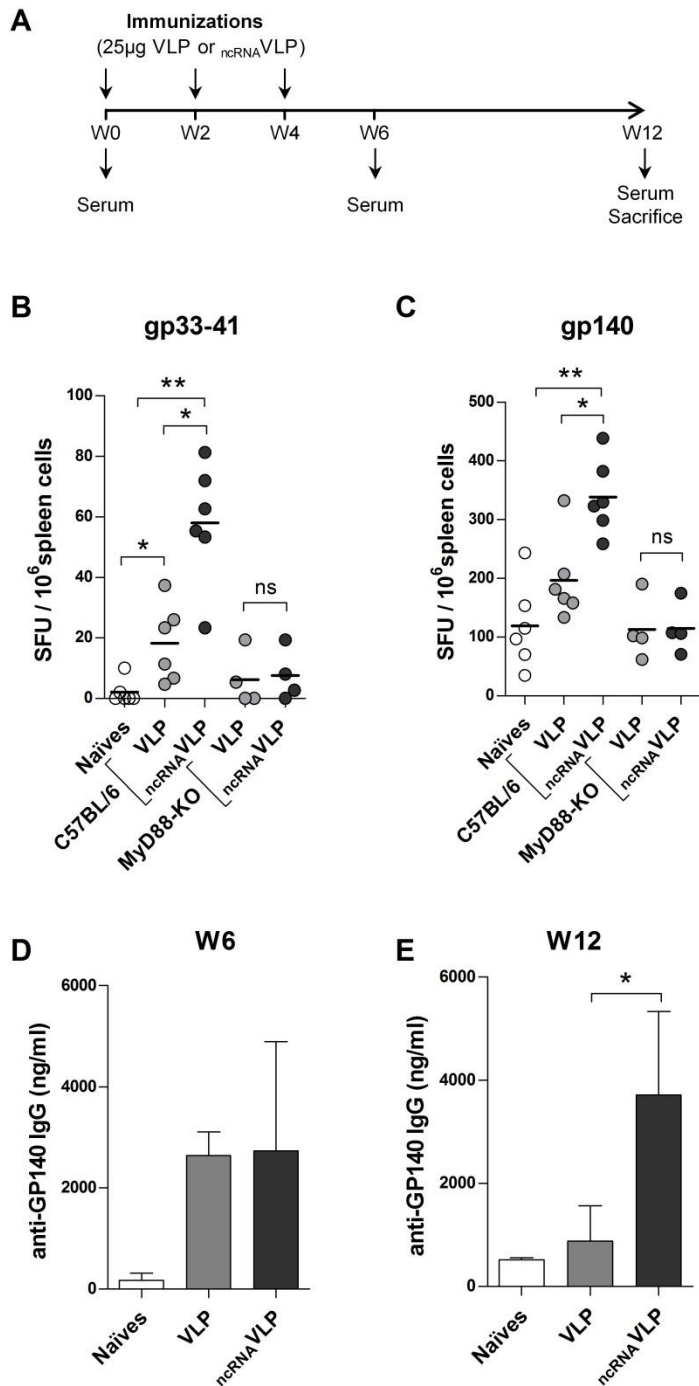


Figure 5:

T- and B-cell immune responses in mice vaccinated with HIV-pseudotyped VLPs carrying or not *ncRNA*. (A) Schematic representation of the vaccination protocol. C57BL/6 or MyD88^{-/-} mice (n = 5 per group) were immunized 3 times at two-week intervals with 25 µg of HIV-pseudotyped Gag-gp33-41 VLPs or *ncRNA* VLPs. Sera were collected from blood samples at weeks 6 and 12. (B, C) Cellular responses were evaluated at week 12 by standard IFN-γ ELISPOT after specific restimulation with either gp33-41 (B) or HIV-gp140 (C). Results represent individual values and group means expressed as number of spot forming units (SFUs) per million of splenocytes. (D, E) Specific anti-gp140 antibody concentrations were evaluated in serum of immunized or naïve C57BL/6 mice by anti-GP120 ELISA at weeks 6 (D) and 12 (E). Results represent the mean values + SEM of measured concentrations. * p ≤ 0.05, ** p ≤ 0.01; Mann-Whitney test.